Author(s): Tyunina, M. & Narkilahti, J. & Plekh, M. & Oja, R. & Nieminen, Risto M. & Dejneka, A. & Trepakov, V.

Title: Evidence for Strain-Induced Ferroelectric Order in Epitaxial Thin-Film KTaO3

Year: 2010

Version: Final published version

Please cite the original version:

Tyunina, M. & Narkilahti, J. & Plekh, M. & Oja, R. & Nieminen, Risto M. & Dejneka, A. & Trepakov, V. 2010. Evidence for Strain-Induced Ferroelectric Order in Epitaxial Thin-Film KTaO3. Physical Review Letters. Volume 104, Issue 22. 227601/1-4. ISSN 0031-9007 (printed). DOI: 10.1103/physrevlett.104.227601.

Evidence for Strain-Induced Ferroelectric Order in Epitaxial Thin-Film $KTaO_3$

M. Tyunina,[1] J. Narkilahti,[1] M. Plekh,[1] R. Oja,[2] R. M. Nieminen,[2] A. Dejneka,[3] and V. Trepakov[3,4]

[1]*Microelectronics and Materials Physics Laboratories, University of Oulu, P.O. Box 4500, FI-90014 Oulun yliopisto, Finland*
[2]*COMP/Applied Physics, Aalto University School of Science and Technology, P.O. Box 11100, FI-00076 Aalto, Finland*
[3]*Institute of Physics, Academy of Sciences of the Czech Republic, Na Slovance 2, 182 21 Prague 8, Czech Republic*
[4]*Ioffe Physical-Technical Institute of the RAS, 194 021 St. Petersburg, Russia*

(Received 31 January 2010; published 1 June 2010)

In perovskite-structure epitaxial films, it has been theoretically predicted that the polarization and the coherence of polar order can increase with increasing crystallographic strain. Experimental evidence of strain-induced long-range ferroelectric order has not been obtained thus far, posing the fundamental question of whether or not strain can induce the long-range polar order. Here we demonstrate the existence of strain-induced ferroelectric order in quantum paraelectric $KTaO_3$ by combining experimental investigations of epitaxial $KTaO_3$ films and density-functional-theory calculations. The long-range ferroelectric order does exist under a large enough epitaxial strain. We suggest that a region of short-range polar order might appear between paraelectric and ferroelectric states in the strain-temperature phase diagrams.

DOI: 10.1103/PhysRevLett.104.227601 PACS numbers: 77.80.−e, 77.55.fp, 77.55.Px, 77.90.+k

Transition-metal oxides exhibit a full spectrum of electronic properties from insulating to semiconducting, metallic, and superconducting. Many of them are ferroics possessing long-range order of magnetic spins (ferromagnets) or electric dipoles (ferroelectrics) or both (multiferroics). Such a spectacular variation in behavior is related to the large effects on electronic structure and ferroic order parameters caused by small changes in atomic positions and crystal structure. In these systems, knowledge-based engineering of novel physical properties able to lead to application breakthroughs is at the cutting edge of solid-state research. Of special practical interest is the possibility to obtain the desired ferroic properties by controlling crystallographic strain [1–5]. The strain control can be realized using heteroepitaxial films, where due to the mismatch of the in-plane (parallel to the substrate surface) lattice parameters of the film material and the substrate, a misfit strain s arises.

In epitaxial thin-film perovskite ferroelectrics (FEs), the biaxial in-plane strain affects the polarization P. The strain-temperature (s-T) phase diagrams of such films have been calculated using both phenomenological and first-principles models [1,3–5]. Compared to bulk unstressed FEs, the increase of the FE transition temperature with increasing strain magnitude $|s|$ and appearance of new crystal and FE phases have been theoretically predicted. Moreover, a strain-induced onset of long-range FE order has been predicted for thin films of the quantum paraelectric strontium titanate ($SrTiO_3$) [2,4,5], which in its chemically pure, stress-free bulk form is not FE at any temperature down to 0 K.

In agreement with modeling studies, in strained films [6] of perovskite-structure FEs, the shift of phase transition temperatures and the enhanced polarization have been experimentally obtained [7,8]. However, in epitaxial films of $SrTiO_3$, in contrast to the predicted long-range FE order, relaxorlike behavior has been experimentally proved [9]. In relaxor ferroelectrics, or relaxors, long-range FE polarization order and FE domains are absent. Local, nanosized clusters of randomly oriented polarization are responsible for the relaxor properties [10]. The nature of polar clusters and their contribution to the extraordinary dielectric and piezoelectric coefficients of relaxors are subjects of continuing research. In contrast to FEs, in relaxors with short-range order of polarization, a peak in the temperature dependence of the dielectric permittivity is not associated with the paraelectric-to-FE phase transition. In $SrTiO_3$ films, the dielectric peak [5] is of relaxor nature [9]. Importantly, in epitaxial films of perovskite-type relaxors, strain has been found to enhance relaxor features, but not to induce the FE state [11]. Unexpectedly, the relaxorlike properties have been observed also in epitaxial films of FE $BaTiO_3$ and FE (Ba, Sr)TiO_3 [12,13].

The question of fundamental importance, can FE order be induced by epitaxial strain, thus remains open. Here we answer this question, based on studies of strained epitaxial $KTaO_3$ (KTO) films. In bulk form, KTO possesses a perovskite-type cubic crystal structure and exhibits paraelectric behavior to the lowest temperatures [14]. We demonstrate the existence of strain-induced FE order in quantum paraelectric KTO by combining experimental investigations of epitaxial KTO films and density-functional-theory (DFT) calculations.

The first-principles analysis of the ground-state structure and polarization in KTO was performed using the DFT calculations with the Vienna *ab initio* simulation package (VASP) [15] and the local density approximation (LDA). The core states were represented using the projector-augmented-wave method [16], and the semicore states of K and Ta were treated as valence electrons. The plane-wave

cutoff energy was 700 eV. For the bulk crystal cubic phase of KTO the LDA equilibrium lattice constant of 3.96 Å was obtained.

To simulate the film, the in-plane epitaxial strain for repeated unit cells of KTO was varied from −2.5% (compressive strain) to 2.5% (tensile strain) by changing the in-plane lattice constants (along X and Y axes). The possible symmetry groups obtained by relaxing ionic positions and out-of-plane lattice constant (along Z axis) are $P4mm$, $Amm2$, and $Pmm2$, with different directions of polarization and phase transition from the nonpolar $P4/mmm$ symmetry. The internal energies of these phases and the ionic displacements in the lowest energy phase are functions of strain [Fig. 1]. For strain $-1\% < s < 0.5\%$, all phases yield the paraelectric $P4/mmm$ structure, which is broken at larger $|s|$. Increasing tensile strain leads to the $Amm2$ structure with the in-plane polarization $P_x = P_y \neq 0$. At large enough compressive strains, the symmetry is lowered to $P4mm$, with the out-of-plane polarization $P_z \neq 0$. Interestingly, a similar sequence of strain-induced phases has been previously obtained for $SrTiO_3$ [4], with the paraelectric gap in a narrower range of $|s| < 0.2\%$.

In compressively strained KTO films with $s < -1\%$, a tetragonal-type FE phase is thus expected. Such films were grown by *in situ* pulsed laser deposition on conducting $SrTiO_3(001)$ single-crystal substrates. To sustain strain without relaxation, a KTO thickness of about 10 nm was selected [17]. The crystal structure of the films was studied by x-ray diffraction as described in Ref. [17]. KTO films grown under optimized conditions are perovskite, with the (001) planes parallel to the substrate surface, and with the epitaxial relationship KTO [100](001) ∥ $SrTiO_3$[100]× (001) [Fig. 2]. In the Θ-2Θ patterns, the peaks of the Laue function due to the small thickness of high-quality smooth crystalline films are seen as satellites around (001) and (002) perovskite reflections [Fig. 2(b)]. The film thickness $d = 9$ nm is determined from the positions of the minima of the Laue function. The in-plane strain is defined as $s_{KTO} = (a_{KTO} - a_0)/a_0$, where a_{KTO} is the in-plane lattice parameter of the KTO film and a_0 is the lattice parameter of bulk KTO. The strain is compressive $s_{KTO} = -2.1 \pm 0.03\%$, with the parameter $a_{KTO} = 3.905 \pm 0.001$ Å being similar to that of the substrate. The out-of-plane lattice parameter of KTO film is $c_{KTO} = 4.008 \pm 0.0005$ Å.

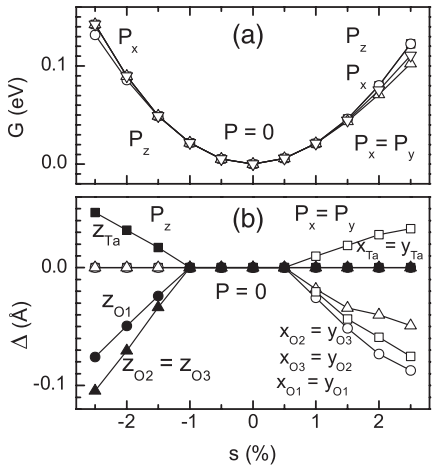

FIG. 1. First-principles analysis of strained $KTaO_3$. Calculated (a) internal energies G of the considered phases and (b) ionic displacements Δ (relative to K ions) in the phase of lowest internal energy as a function of in-plane strain s. In (b), solid symbols indicate out-of-plane displacements and open symbols indicate in-plane displacements.

In ultrathin films, experimental identification of FE state is not a trivial task. To prove FE transition in the deposited KTO films, several methods and comparison with different systems were applied. The dielectric response of vertical capacitor structures KTO/$SrTiO_3$ with Pt top electrodes was measured using an HP 4284A LCR meter. Since extrinsic contributions to the measured capacitance C are not exactly known [18,19], the real part of the dielectric permittivity of the KTO film cannot be accurately determined. However, its evolution as a function of temperature and electric field can be followed by analyzing the measured capacitance density C/S, where S is the area of the top electrode pad.

In the compressively strained KTO film, the temperature dependence of the dielectric permittivity is completely different from that in bulk KTO [14]: the dielectric peak is found at $T_m \approx 760$ K, similar for both the capacitance density and the loss factor tan$D$ [Fig. 3(a)]. The frequency dispersion of the measured tan$D$ and C/S is due to capacitor design [19]. The relaxorlike frequency dependence of T_m is not detected, implying the FE character of transition.

To prove the FE behavior below T_m, the shape of the dielectric peak is analyzed using the derivative $\xi(T)$ of inverse permittivity [12,20] (or that of inverse capacitance density) [Fig. 3(b)]. In relaxor $PbMg_{1/3}Nb_{2/3}O_3$, the derivative $\xi(T)$ decreases with decreasing T below T_m [20]. Similar behavior is found in relaxorlike $BaTiO_3$ films [12]. Importantly, in normal FEs, the derivative $\xi(T)$ increases weakly on cooling below T_m [Fig. 3(c)], tending to the low-temperature Curie-Weiss behavior. Despite the broadening of the dielectric peak, typical for vertical FE thin-film capacitors, the observed increase of $\xi(T)$ in the KTO film [Fig. 3(b)] is similar to normal FE.

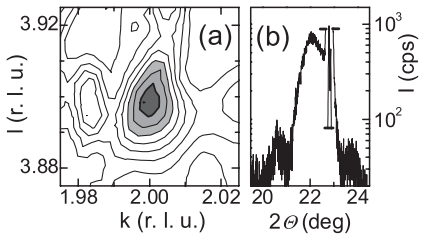

FIG. 2. Crystal structure of $KTaO_3$ film. (a) Reciprocal space map of the film around (024) reflections on the (0kl) $SrTiO_3$ reciprocal lattice plane. (b) Θ-2Θ x-ray diffraction pattern around perovskite (001) reflection of the film. Intensity of the substrate reflection is reduced by filtering.

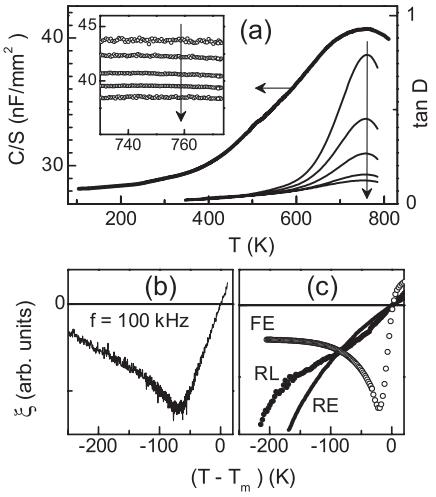

FIG. 3. Dielectric response of the $KTaO_3$ thin-film capacitor. (a) Capacitance density C/S ($f = 50$ kHz) and loss factor tan$D$ ($f = 5$, 20, 50, and 200 kHz) as a function of temperature T. Inset shows C/S ($f = 5$, 10, 20, 50, and 100 kHz) around T_m. Arrows show direction of increase of f. (b) Derivative ξ as a function of normalized temperature ($T - T_m$) in (b) $KTaO_3$ film compared to those in (c) 350 nm thick relaxor film of $PbMg_{1/3}Nb_{2/3}O_3$ (RE) [20], 400 nm thick relaxorlike film of $BaTiO_3$ (RL) [12], and bulk ferroelectric $Pb_{0.5}Sr_{0.5}TiO_3$ ceramic (FE). The measurement frequency f is 100 kHz.

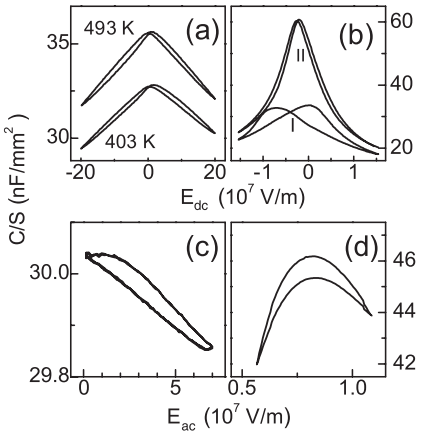

FIG. 4. Nonlinear dielectric behavior in the $KTaO_3$ thin-film capacitor. Capacitance density C/S (at $f = 20$ kHz) as a function of (a),(b) applied dc electric field E_{dc} and (c),(d) amplitude E_{ac} of ac electric field measured in (a),(c) the $KTaO_3$ film and (b),(d) 130 nm thick film of FE $Pb_{0.5}Sr_{0.5}TiO_3$ at $T = 300$ K ($T_m = 420$ K) and (b) $E_{ac} = 100$ kV/m (curve I) and 10 MV/m (curve II).

The FE state is characterized by the presence of polarization P that can be switched by applied dc electric field E_{dc}. In vertical capacitors of ultrathin FE films, the measurement of quasistatic P-E_{dc} loops is limited by an exponential increase of injection current with increasing E_{dc} [21]. Dynamic loops, often studied instead, look similar in FE and relaxor films due to frequency dependent relaxor response and thus are not suitable for proving the FE state. In the prepared KTO films, the FE hysteresis is revealed in the field dependence C/S (E_{dc}) measured by sweeping E_{dc} superimposed with the probing ac electric field [Fig. 4(a)]. The FE shape of hysteresis looks distorted since the amplitude E_{ac} is large due to very small film thickness ($E_{ac} \sim 1$ MV/m). Note that similar distortion is seen in an epitaxial film of normal FE $Pb_{0.5}Sr_{0.5}TiO_3$ [Fig. 4(b)]: the typical butterflylike FE hysteresis is obtained at smaller E_{ac} (100 kV/m) and it is distorted at larger E_{ac}.

The low-frequency dynamics of the FE domains and polar clusters are principally different. In thin films, the difference is well seen in the dependence of the response on amplitude E_{ac} of ac electric field, C/S (E_{ac}) [22]. This can be used to reveal the presence of FE domains. The observed hysteresis C/S (E_{ac}) [Fig. 4(c)] is in contrast to the hysteresis-free behavior typical for relaxor films and is similar to that in FE films at very large field E_{AC} [compare with Fig. 4(d)]. This provides further evidence for the FE state in the KTO films.

In ferroics, phase transitions can be detected by studying the temperature dependence of optical index of refraction $n(T)$. This is due to coupling between refraction variation δn and ferroic order parameter [23]. In FE at $T < T_m$, spontaneous polarization P_s gives contribution to n via electro-optic effect: $\delta n = -1/2n\gamma\langle P_s\rangle^2$, where γ is electro-optic coefficient. In the grown KTO film without top electrodes, the effective index of refraction was determined using ellipsometry techniques [24] at wavelength $\lambda = 500$ nm. The obtained dependence $n(T)$ [Fig. 5(a)] dramatically differs from a weak monotonic increase of n observed on cooling in single-crystal KTO [24]. It is also in contrast to the optical properties of relaxors [25]. The shape of $n(T)$ in Fig. 5(a) is remarkably similar to that in single-crystal $BaTiO_3$ in the vicinity of paraelectric-to-FE phase transition [14].

In the FE KTO films, the temperature T_m of the FE phase transition estimated from $n(T)$ is around 700 K, lower than $T_m \approx 760$ K found from the dielectric measurements. The difference is due to different boundary conditions, which are (i) open circuit conditions with an unscreened depolarizing field for the measurements of $n(T)$ and (ii) short circuit conditions with a partial screening of depolarizing field for the dielectric measurements. The transition temperatures obtained in (i) and (ii) reveal the minor role of the

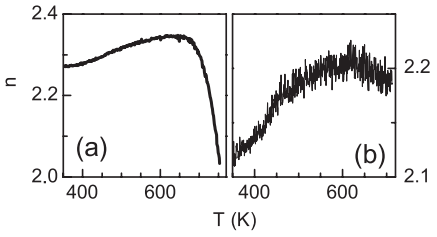

FIG. 5. Ferroelectric-type optical behavior. Optical index of refraction n as a function of temperature T in strained epitaxial films of (a) $KTaO_3$ with compressive strain 2.1% and (b) $SrTiO_3$ with tensile strain 2.1%.

boundary conditions at the KTO film surfaces [26] on the onset of FE state. The main reason for the FE transition in KTO film is strain.

In the studied KTO films, the high-temperature FE transition is experimentally proved by the low-frequency dielectric peak with frequency independent T_m, tendency to low-temperature Curie-Weiss behavior, FE-type dielectric nonlinearity, and FE-type temperature variation of optical index of refraction. Thus the long-range FE order exists in the epitaxial films of quantum paraelectric KTO with the in-plane compressive strain $s = -2.1\%$, the magnitude of which is beyond the theoretical paraelectric gap (Fig. 1). This differs from the relaxorlike state in epitaxial films of quantum paraelectric $SrTiO_3$ with the in-plane tensile strain $s \approx 1\%$ [9], also well beyond the theoretical paraelectric gap [4,5]. To demonstrate that strain-induced FE order is characteristic not only for KTO or compressive strain, we show here the temperature dependence of refraction index $n(T)$ measured in epitaxial film of $SrTiO_3$ with the in-plane tensile strain $s = 2.1\%$. (The crystal structure and the room-temperature optical properties of epitaxial $SrTiO_3$ films have been studied in our recent work [17].) The FE-type $n(T)$ in Fig. 5(b) evidences that strain-induced FE order exists also in $SrTiO_3$ and at tensile strain, if the strain magnitude is sufficiently large. Importantly, in the $SrTiO_3$ film with $s = 0.85\%$, the FE-type anomaly in $n(T)$ is not found.

In epitaxial KTO and $SrTiO_3$ films, the long-range FE order exists if the strain magnitude considerably exceeds the predicted paraelectric boundary. In the (s-T) phase diagrams, a region of short-range polar order might exist between the paraelectric and long-range ordered FE states. Such a region might also exist in epitaxial films of FE $BaTiO_3$. In $BaTiO_3$ films, the FE order has been demonstrated for $s = -2.1\%$ [8], $s = -1.3\%$ [7], and $s = 0.58\%$ [27], with the relaxorlike properties found for $s = -0.7\%$–0% [12]. The relaxorlike properties evidenced in epitaxial films of (Ba, Sr)TiO_3 [13] indicate a presence of the short-range-order region in the phase diagram for this FE, too. Similar short-range order found in epitaxial films grown by different methods and in different laboratories [9,12,13] suggests its fundamental origin, not related to technological imperfections. Studies of dynamic effects might give a clue to understanding this origin [12,28]. The current static strain-polarization concept is not sufficient.

In conclusion, we have proved that strain-induced long-range ferroelectric order exists in perovskite-structure quantum paraelectrics under a large enough epitaxial strain. Understanding the phase diagrams of epitaxially grown ferroic films remains a challenge.

This research has been supported by the Academy of Finland through the FERNAND consortium of the FinNano Programme as well as the Centers of Excellence Programme (2006—2011) and by Czech Academy of Science (AV0Z10100522, KAN301370701).

[1] N. A. Pertsev, A. G. Zembilgotov, and A. K. Tagantsev, Phys. Rev. Lett. **80**, 1988 (1998); N. A. Pertsev, Phys. Rev. B **78**, 212102 (2008).
[2] N. A. Pertsev, A. K. Tagantsev, and N. Setter, Phys. Rev. B **61**, R825 (2000).
[3] O. Dieguez *et al.*, Phys. Rev. B **69**, 212101 (2004).
[4] O. Diéguez, K. M. Rabe, and D. Vanderbilt, Phys. Rev. B **72**, 144101 (2005).
[5] J. H. Haeni *et al.*, Nature (London) **430**, 758 (2004).
[6] S. M. Yang *et al.*, J. Korean Phys. Soc. **55**, 820 (2009); W. Hong *et al.*, Phys. Rev. Lett. **95**, 095501 (2005).
[7] K. J. Choi *et al.*, Science **306**, 1005 (2004).
[8] D. A. Tenne *et al.*, Phys. Rev. Lett. **103**, 177601 (2009).
[9] M. D. Biegalski *et al.*, Appl. Phys. Lett. **88**, 192907 (2006); Phys. Rev. B **79**, 224117 (2009).
[10] G. Xu *et al.*, Nature Mater. **7**, 562 (2008); Z. Kutnjak, J. Petzelt, and R. Blinc, Nature (London) **441**, 956 (2006).
[11] M. Tyunina, J. Levoska, and S. Leppävuori, J. Appl. Phys. **91**, 9277 (2002); M. Tyunina and J. Levoska, J. Appl. Phys. **97**, 114107 (2005).
[12] M. Tyunina, J. Levoska, and I. Jaakola, Phys. Rev. B **75**, 140102(R) (2007).
[13] M. Tyunina and J. Levoska, Phys. Rev. B **70**, 132105 (2004); D. A. Tenne *et al.*, Phys. Rev. B **67**, 012302 (2003).
[14] *Numerical Data and Functional Relationships in Science and Technology*, edited by K. H. Hellwege and A. M. Hellwege, Landolt-Bornstein, New Series, Group III, Vol. 16 (Springer, Berlin, 1981).
[15] G. Kresse and J. Hafner, Phys. Rev. B **48**, 13115 (1993); G. Kresse and J. Furthmüller, Phys. Rev. B **54**, 11 169 (1996).
[16] P. E. Blöchl, Phys. Rev. B **50**, 17 953 (1994); G. Kresse and D. Joubert, Phys. Rev. B **59**, 1758 (1999).
[17] M. Tyunina *et al.*, J. Phys. Condens. Matter **21**, 232203 (2009).
[18] M. Stengel, D. Vanderbilt, and N. A. Spaldin, Nature Mater. **8**, 392 (2009).
[19] M. Tyunina, J. Phys. Condens. Matter **18**, 5725 (2006).
[20] M. Tyunina, M. Plekh, and J. Levoska, Phys. Rev. B **79**, 054105 (2009).
[21] L. Pintilie *et al.*, Phys. Rev. B **75**, 104103 (2007).
[22] M. Tyunina, J. Levoska, and I. Jaakola, Phys. Rev. B **74**, 104112 (2006); M. Tyunina, M. Plekh, and J. Levoska, Ferroelectrics **373**, 44 (2008).
[23] J. Fousek and J. Petzelt, Phys. Status Solidi A **55**, 11 (1979); R. V. Pisarev *et al.*, Phys. Rev. B **28**, 2677 (1983); M. E. Guzhva, P. A. Markovin, and W. Kleemann, Phys. Solid State **39**, 625 (1997); P. A. Markovin *et al.*, JETP Lett. **86**, 712 (2008).
[24] W. Kleemann and F. J. Shaefer, Jpn. J. Appl. Phys. **24**, 260 (1985); V. Trepakov *et al.*, New J. Phys. **11**, 083024 (2009).
[25] A. E. Krumin, U. Y. Ilyin, and V. I. Dimza, Ferroelectrics **22**, 695 (1978).
[26] A. R. Akbarzadeh *et al.*, Appl. Phys. Lett. **90**, 242918 (2007).
[27] D. A. Tenne *et al.*, Phys. Rev. B **69**, 174101 (2004).
[28] J. Hlinka *et al.*, Phys. Rev. Lett. **101**, 167402 (2008).